



An estimate of energy dissipation due to soil-moisture hysteresis

by

H. McNamara

An estimate of energy dissipation due to soil-moisture hysteresis

H. McNamara^{*}

July 16, 2012

Abstract

Processes of infiltration, transport and outflow in unsaturated soil necessarily involve the dissipation of energy through various processes. Accounting for these energetic processes can contribute to modelling hydrological and ecological systems. The well-documented hysteretic relationship between matric potential and moisture content in soil suggests that one such mechanism of energy dissipation is associated with the cycling between wetting and drying processes. Working from a time-series of soil moisture content data (taken in the south-west of Ireland), and making rather straightforward assumptions regarding the hysteretic relationship mentioned, the average rate of energy dissipation was found to be $O(10^{-5})$.

1 Introduction

The hysteretic relationship between soil-matric potential and moisture content has been studied since at least 1930, when its identification by W.B. Haines settled an academic disagreement he had with the well known statistician R.A. Fisher, (*Haines*, 1925; *Fisher*, 1926; *Haines*, 1927, 1930). The essence of this relationship is the fact that less mechanical energy is required to make dry soil wet than to make that wet soil dry, and it is key to a large number of processes and systems — it is arguable that agriculture would not be possible without this mechanism for trapping water close to the surface of the soil layer. A schematic of the matric potential-moisture content relationship is shown in figure 1.

^{*}Oxford Centre for Collaborative Applied Mathematics and Oxford Martin School, University of Oxford, UK.

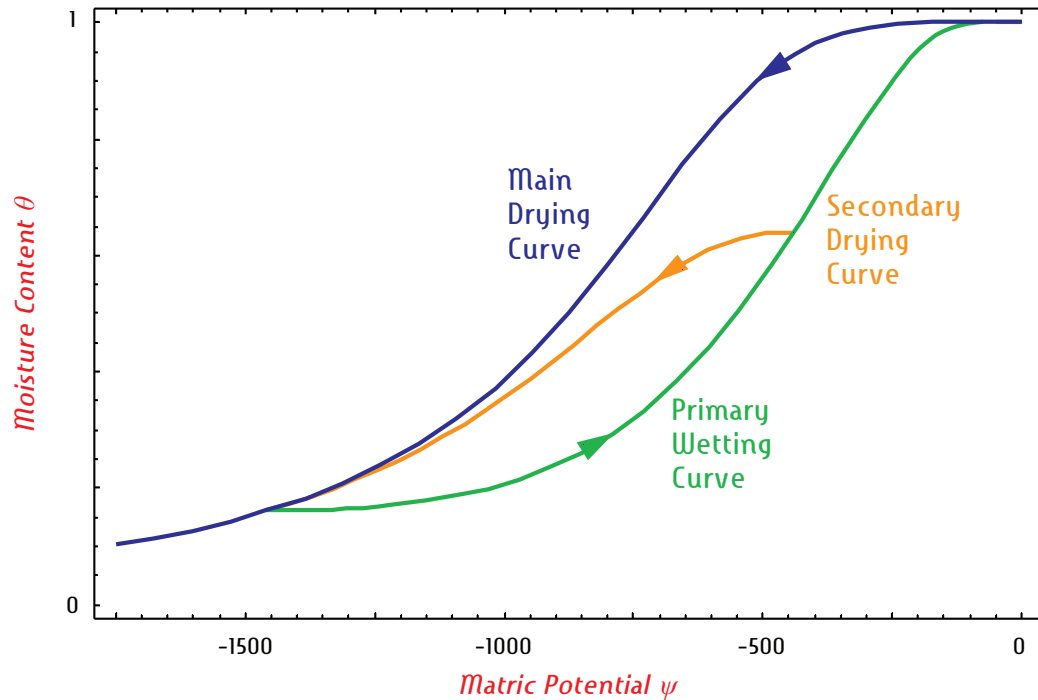


Figure 1: A schematic of the hysteretic relationship between matric potential and moisture content in unsaturated soils. Shown are the *main drying curve*, taken when moisture content decreases monotonically from saturation, and two reversal curves — a primary wetting curve and an associated secondary drying curve.

The description and modelling of soil-water hysteresis developed through a number of stages, mirroring in some respects, and interacting with, the development of models of ferromagnetic and adsorption hysteresis during the same time period (the introduction to *Mayergoyz, 2003*, and a sidebar in *Appelbe et al., 2009*, contain some details and good references for tracing this history). A comprehensive mathematical treatment of hysteresis phenomena in general was undertaken in the 1970s and 80s by a group of Russian mathematicians under Mark Krasnosel'skii, and it was realised that a new mathematical idea was underlying the various models which had arisen in diverse physical settings. The publication, and later the translation into English, of the seminal monograph by *Krasnosel'skii and Pokrovskii (1989)* triggered a large volume of work on hysteresis operators, and their use in dynamical systems, control theory and differential equations; in many fields, theoretical and applied (key publications include *Mayergoyz, 1991*; *Visintin, 1993, 1994*; *Brokate and Sprekels, 1996*; *Mayergoyz, 2003*; *Bertotti and Mayergoyz, 2006*).

Hysteresis in fluid flow through porous media is explained as resulting from the capillary behaviour in small pore spaces and channels. These effects are incorporated

into many models of porous flow, for example those commonly used in petroleum reservoir simulation, (for example *Morrow and Harris*, 1965; *Kleppe et al.*, 1997; *Hustad*, 2002), which do not share the Krasnosel'skii approach to hysteresis phenomena, and many which do, (such as *Bagagiolo and Visintin*, 2000; *Hanyga and Seredyńska*, 2005; *Lamacz et al.*, 2011). None of these, however, address the specific issue of energy dissipation due to capillary hysteresis.

An application of the *Preisach model* (*Preisach*, 1935; *Mayergoyz*, 2003) to soil-water hysteresis by *Flynn et al.* (2006), undertaken in Cork, Ireland in recent years using the GRIZZLY database of experimental results, (*Haverkamp et al.*, 2002), provided a simple family of Preisach models with a good track-record of fitting soil-water data. The approach taken was to build on empirical work previously undertaken to characterise the shape of the main drying curve in *Haverkamp et al.* (2002), and to use a single extra parameter in the description of the Preisach distribution function. This resulted in improved fits to empirical data. Further work by the same group included the use of Preisach hysteresis in a model of the interaction between rainfall, biomass and soil-water dynamics, which has also shown good agreement with data, (an overview of all this work is in *Appelbe et al.*, 2009).

One of the outcomes of the modelling process described in *Appelbe et al.* (2009) is a procedure for estimating the hysteretic properties of soil from combined moisture-content and rainfall data. The same data is used in this work, being taken over a period of 19 months from July 2002 to February 2004 from a location in Kerry in south-west Ireland. Energy dissipation in the soil-water system was considered in *Brokate et al.* (2011) using the rainfall data and the model described in *Appelbe et al.* (2009). This work can be seen as a companion piece, in that the other portion of the data is used directly (moisture content). The different set of assumptions made here work as an independent check on the results obtained there.

1.1 The Preisach Nonlinearity

The hysteresis model introduced by Ferenc Preisach 1935, is increasingly important in the modelling of various hysteretic systems. Although introduced to describe an electromagnetic phenomenon, it is fundamentally similar to the Independent Domain Model for soil-moisture hysteresis, and has been applied to phenomena in various fields. A reason for the relative popularity of the Preisach model is that it admits a rather natural algorithmic description. This also facilitates its implementation in numerical models using differential equations. A full description of the Preisach model is not given here, the interested reader is referred to the references mentioned earlier, and to the online demonstration (*Flynn et al.*, accessed 3 July 2012). The important aspect here is the geometric interpretation, which is briefly

summarised.

The Preisach model (or Preisach nonlinearity, Preisach operator) relates an input function, $u(t)$, to an output function $v(t)$. The relationship is fundamentally *non-local*: for a given function $u(t)$, $t > t_0$, the pair $(u(t_0), v(t_0))$ does not completely determine $v(t)$ for $t > t_0$. Some information about the history of $u(t)$ for $t < t_0$ also contributes to determining $v(t)$. The geometric interpretation of the Preisach model provides a visualisation of this memory.

Consider the half-plane Ω lying above the main diagonal: $\beta > \alpha$. A Preisach state-curve is a (non-strictly) monotone decreasing curve in this half-plane, and divides it into two disjoint portions, Ω_+ and Ω_- , as shown in figure 2. The intersection of this curve with the main diagonal $\alpha = \beta$ is the current value of the input, $u(t)$. As the input varies, it "drags" a segment of the state curve — horizontal if u is increasing, vertical if decreasing — thus transferring points between Ω_- and Ω_+ . This is illustrated in figures 2–4. As a result of these dynamics, after a short time the state curve will have a "staircase" form (at least in a neighbourhood of the main diagonal). The "memory" of the Preisach model consists of *non-dominated extrema* of the input function, and these values mark the "corners" of the staircase. Remembered values can be forgotten, or "wiped-out", which happens when the moving state curve catches up with an earlier turning point. This gives rise to the well-known *return-point memory* property of Preisach hysteresis.

For a wide range of input functions (for example piecewise monotone functions) the memory structure can be written as a finite sequence of these "shock" values $U = \{u_0, u_1, u_2, \dots, u_K\}$, where u_0 is the global maximum of the input, u_1 is the minimum value of the input taken after the global minimum is achieved, u_2 is the maximum value achieved after u_1 , and so on. Two subsequences can thus be identified, $\{u_{2n}\}$ and $\{u_{2n+1}\}$, which correspond to non-dominated maxima and minima respectively. The sequence of maxima (minima) is thus a decreasing (resp. increasing) sequence, bounded from below (above) by the current value of the input function, u_K . If K is even, the input has most recently been increasing, if K is odd it has been decreasing. New shock values, caused by changes in direction of the input, cause an increase in K by 1, and add an entry to the sequence U . If the input value is increasing (K is even), then we have $u_K \leq u_{K-2}$ (excepting the case where $K = 0$). If the input, u_K , exceeds the most recent maximum (u_{K-2}), then both u_{K-1} and u_{K-2} are "wiped-out" and K is decreased by 2.

The output of the Preisach nonlinearity is the measure of the set Ω_- with respect to a suitable measure. In most cases this is expressed as the integral over the set Ω_- of a *Preisach function* $\mu(\alpha, \beta)$, so that the output at an instant t is

$$v(t) = \int_{\Omega_-(t)} \mu(\alpha, \beta) d\alpha d\beta,$$

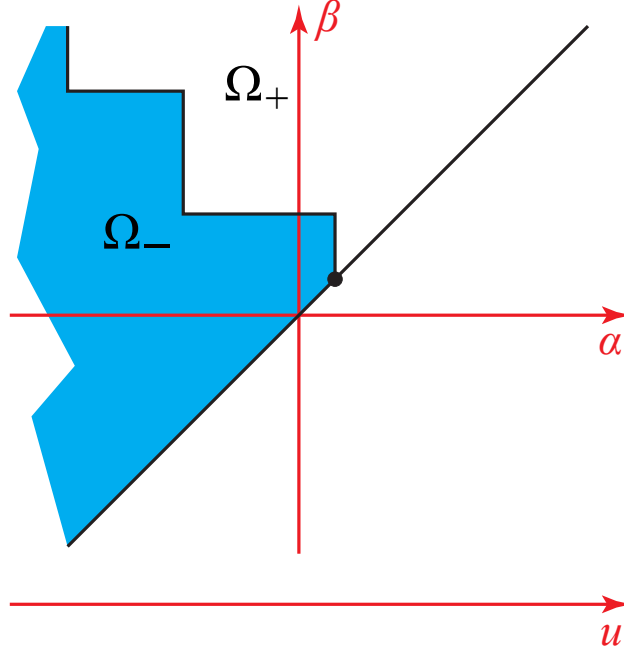


Figure 2: Preisach plane, showing the state curve and the two regions into which the plane Ω is divided.

where the set Ω_- depends on the history of the input $u(\tau)$ for $\tau \leq t$ — in practical applications it depends directly on the sequence of non-dominated extrema U . This algorithmic description of the Preisach model is equivalent to the definition as a parallel connection of non-ideal relays, and to the formulation using the Play operator. For simplicity of notation, the Preisach nonlinearity is written as

$$v(t) = \mathcal{P}[\eta_0, u](t), \quad t \geq t_0$$

where the initial Preisach state at time t_0 is denoted η_0 (assuming that $u(0)$ is compatible with η_0).

Identification of the Preisach function for a given system — for example using experimental soil-moisture and matric potential data — is a nontrivial task, and is not dealt with here. Given an initial state curve at a time t_0 and a Preisach function, the trajectory of points $(u(t), v(t))$, $t > t_0$ (for a large class of reasonable functions $u(t)$) can be determined algorithmically.

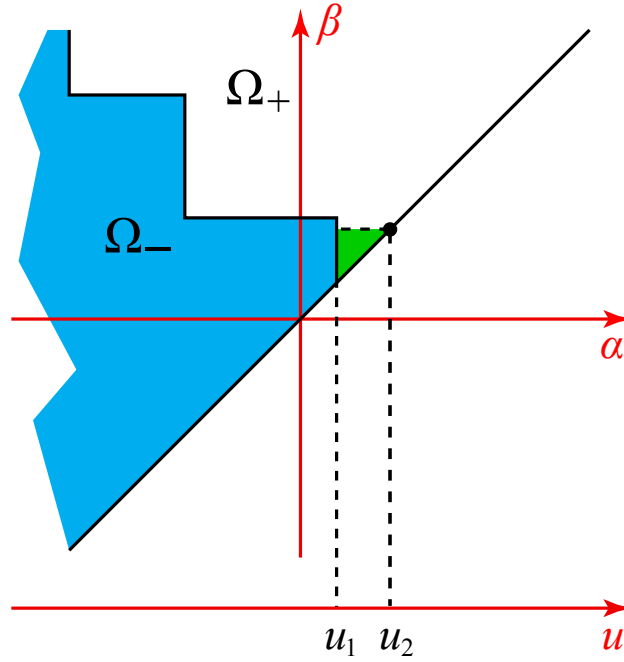


Figure 3: An increase in the input from u_1 to u_2 would "drag" a horizontal line, adding to Ω_- any points it passes. Thus the green region is added to Ω_- .

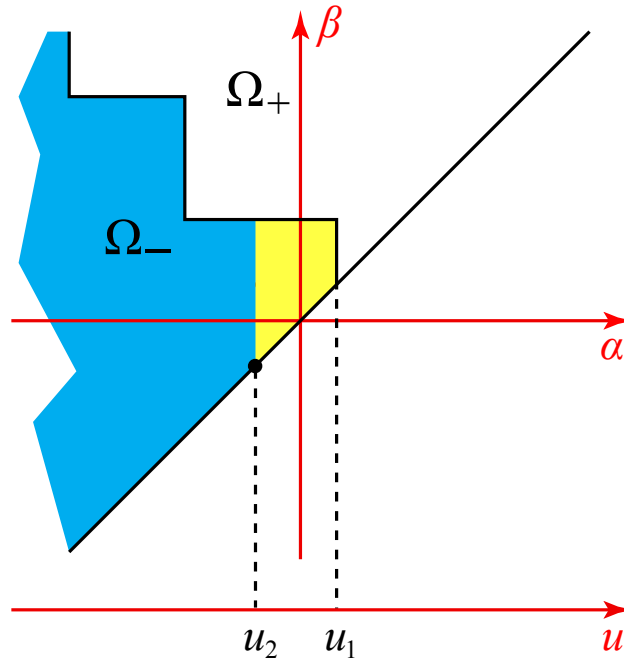


Figure 4: If, instead, the input decreased from u_1 to u_2 , a vertical line would be "dragged", removing points from Ω_- as it passes, shown here in yellow.

1.2 Hysteresis and energy dissipation

Hysteretic processes are fundamentally associated with dissipation. The dissipative nature of hysteresis operators is key to many theoretical results regarding differential systems with hysteresis, see for example *Krejčí* (1996). From an applications perspective, an expression for the amount of energy dissipated can be obtained which holds for arbitrary inputs. A good description can be found in *Mayergoyz* (2003), and a relevant application of this principle is in *Brokate et al.* (2011).

It is worth mentioning here that the dissipation associated with hysteresis is not that of friction or viscosity. Both of these effects are inherently *rate-dependent*, in that the amount of energy dissipated depends on the rate at which changes in the variables occurs. Hysteresis, in contrast, is a *rate-independent* effect. Indeed, the property of rate-independence can be seen as the defining property of hysteresis. The rate-independent component of a relationship can be observed by considering how the system acts under very slow changes in the control/input variable(s). Indeed, that is how many soil-moisture retention curves are obtained, by slowly varying the matric potential and allowing the system to settle for each datum.

In this work, an approximate input-output curve is obtained from time-series moisture data, and this is further used to estimate the rate of hysteretic energy dissipation. The key procedure required for this is approximating matric potential values from soil-moisture data, and this is discussed in the following section. Once this has been carried out, estimating energy dissipation is reasonably straightforward.

2 Data and analysis

Time-series of soil moisture content from the Feale watershed in Co. Kerry, Ireland, was used for this study. Details of the data collection are in *O’Kane and Migliori* (2004). The two time series, from different depths (about 30cm and about 60cm below ground level), cover the time period from August 2002 – February 2004, with a time resolution of one hour, and are shown in figure 5. The same data, along with corresponding rainfall measurements, were used in validating a fully coupled, closed-loop system (the *FEST* model described in *Appelbe et al.*, 2009), part of which involved an identification of a Preisach function suitable for the particular soil type at this location. This Preisach function will be used here, as is the standard notations: θ is the relative moisture content (a value of 1 corresponding to fully saturated soil), which is dimensionless and is the output of the hysteretic relationship (v above); and ψ is the matric potential, the input to the hysteresis nonlinearity, measured in units of length (energy per unit weight of water).

2.1 Inverting the Preisach nonlinearity

As mentioned earlier, the Preisach nonlinearity “remembers” non-dominated extreme values of the input. In order to begin estimating the matric potential from the moisture content, an assumption must be made regarding the initial “memory” of the system. The most straightforward assumption would be that the memory sequence initially consists of a single value — the first measurement. This would certainly be the case if the first measurement was the global maximum — as would be the case here if the soil started out completely saturated. At no point in the measurement interval did the soil become completely saturated ($\theta = 1$), however there is a time early in the data at which the moisture content was very high, and at least close to the maximum attained during the measurement interval. By discarding values taken prior to this point the simple assumption for the initial memory can be justified. The resulting, shorter, time-series should still cover enough time for reliable average rates to be obtained.

From this starting point, a possible time-series for the matric potential is constructed using a simple nonlinear root-finding procedure. From a state η_n and the corresponding input and output values θ_n and ψ_n at time t_n , a value ψ_{n+1} is obtained such that, if $\psi(t)$, $t_n \leq t \leq t_{n+1}$ varies monotonically from ψ_n to ψ_{n+1} , the resulting output value is equal to the next data point, θ_{n+1} , i.e.

$$\theta_{n+1} = \mathcal{P}[\eta_n, \psi](t_{n+1}).$$

The resulting updated state is η_{n+1} and is used for incorporating the next datum. The procedure for finding ψ_n is as follows: to start with, either $\theta_{n+1} \geq \theta_n$ or $\theta_{n+1} < \theta_n$, which of these is the case determines the direction of search for ψ_{n+1} . This direction of search determines the value of $s = \pm 1$, with $s = 1$ if $\theta_{n+1} \geq \theta_n$. A value $\hat{\psi}_{n+1,1} = \psi_n + s\delta$ for some $\delta > 0$, and the corresponding $\hat{\theta}_{n+1,1}$ is found such that $(\theta_n - \theta_{n+1})(\theta_n - \hat{\theta}_{n+1,1}) \leq 0$. The result is an interval $(\psi_n = \hat{\psi}_{n+1,0}, \hat{\psi}_{n+1,1})$ which contains the desired value of ψ_{n+1} . A bisection method proceeds to obtain this value to a chosen precision, and calculates the associated updated Preisach state η_{n+1} .

In carrying out this procedure, the assumption is made that the matric potential (and hence moisture content) varies monotonically between consecutive data points. Little can be done about this potential source of error — the assumption is necessary for all that follows. The time-scales involved in the wetting and drainage/drying processes are shorter than an hour, however the time-scales of variations in precipitation (which drives variation in moisture content) are at least comparable, so that the errors introduced should not be significant.

The reconstructed matric potential series are shown in figure 5 along with the original moisture content data. Figure 7 shows the series in the ψ - θ plane, with a closer

view of a portion of the first series in figure 8.

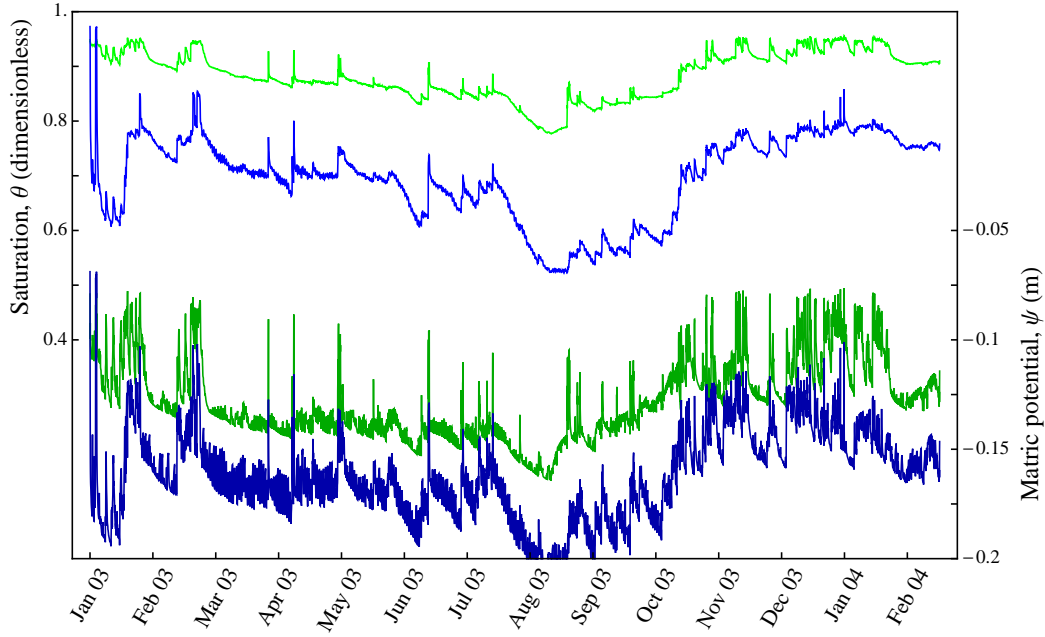


Figure 5: Time series and reconstruction. The top curves show the time-series used in the analysis, with the green curve representing the shallower data. The bottom curves show the reconstructed matric potential, on different axes. An interesting feature of the data is the larger variability in the deeper data. This will have implications for the energy dissipation.

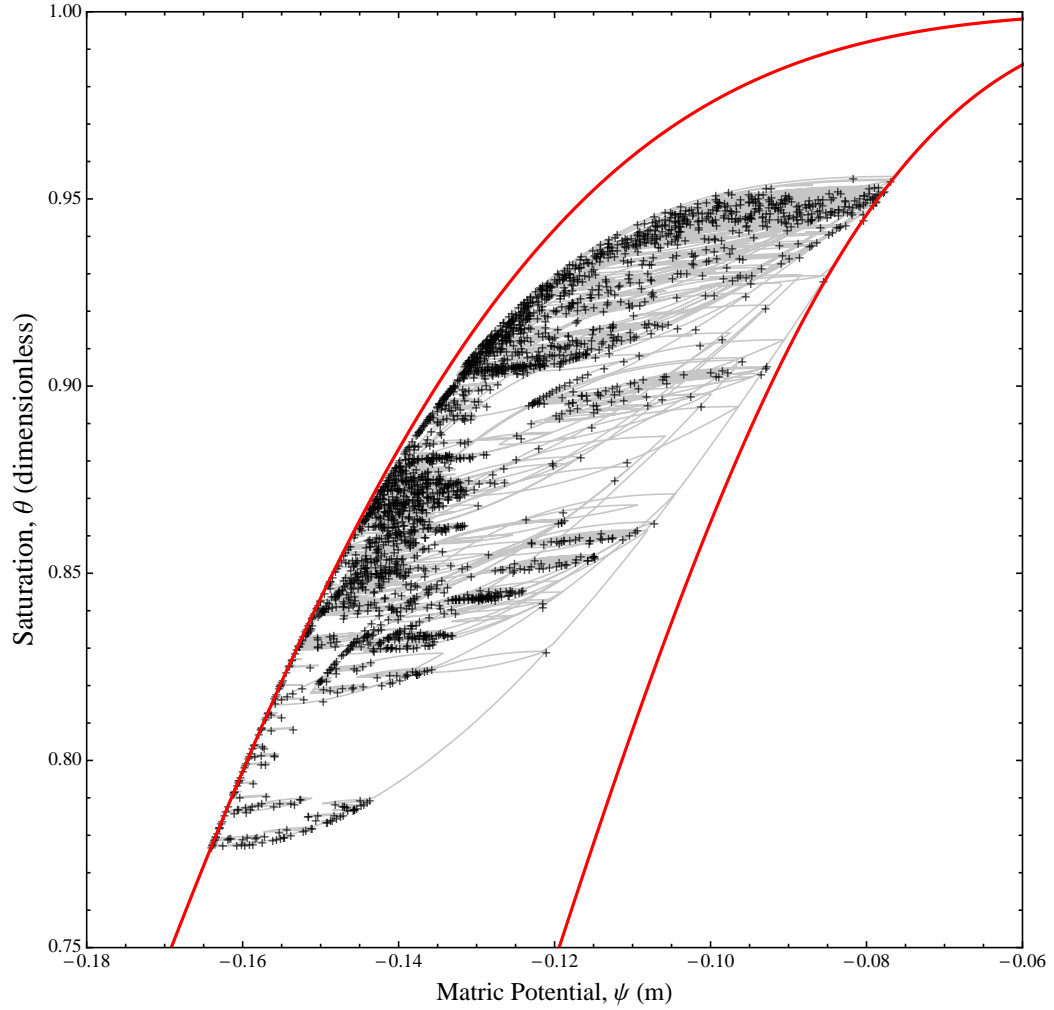


Figure 6: Time series and reconstruction in the ψ - θ plan, first series. The envelope curve shows the main drying and wetting curves. Data points are linked by high-order spanning curves suggested by the analysis.

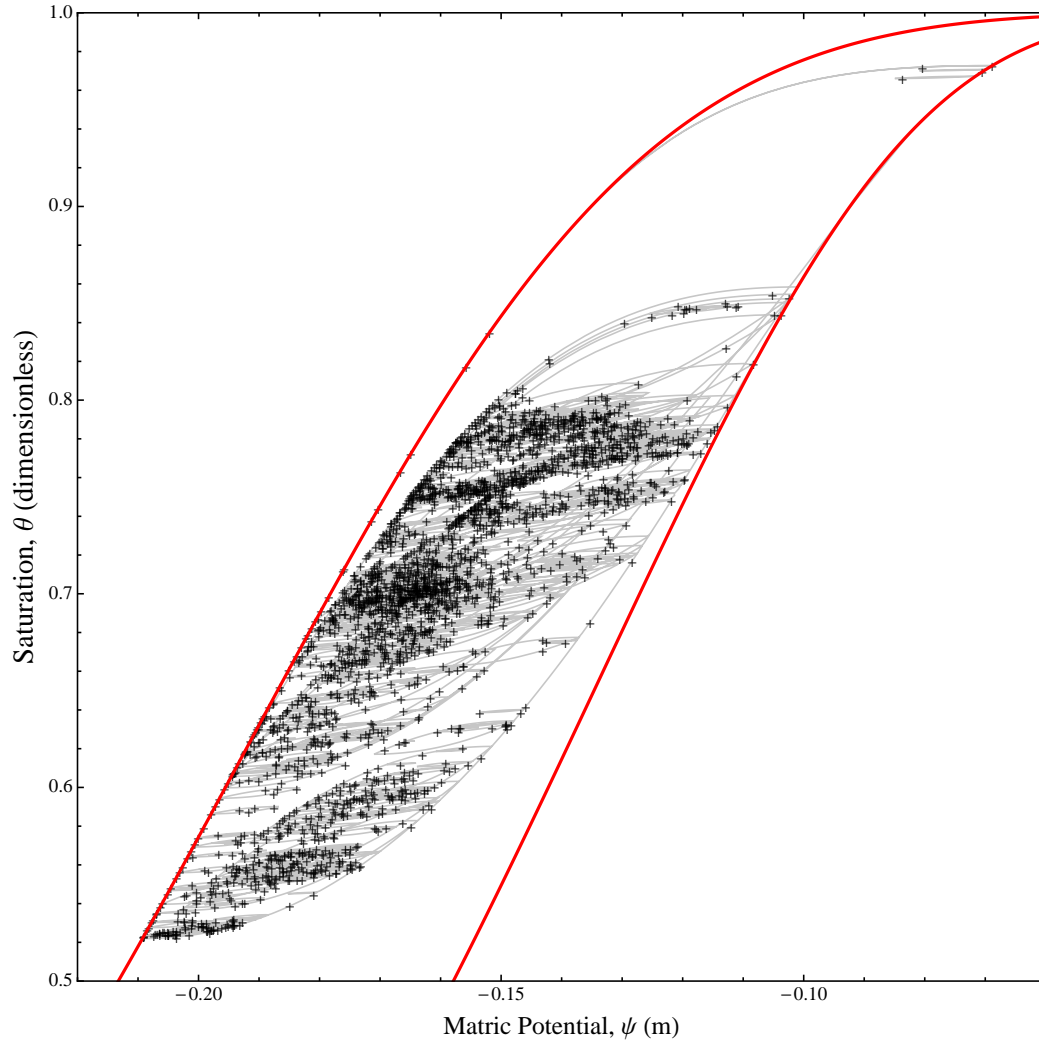


Figure 7: Time series and reconstruction in the ψ - θ plan, second series.

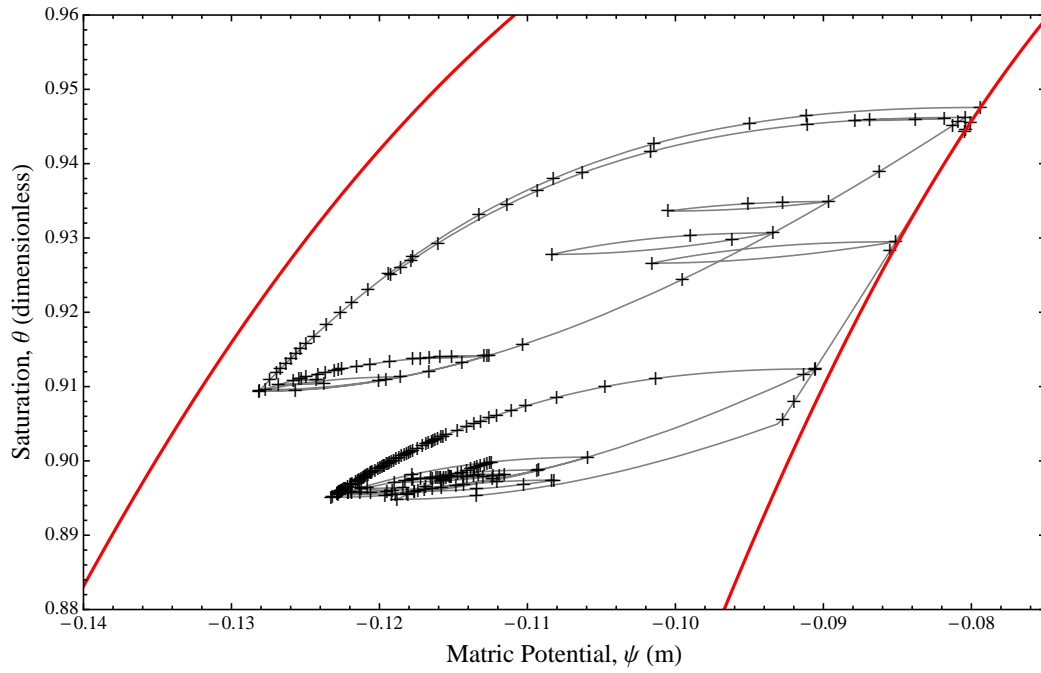


Figure 8: A closer view at a portion of the first time-series/reconstruction. The nesting of smaller loops within larger can be seen.

2.2 Estimating energy dissipation

The work performed on the system in an interval $[0, T]$ can be expressed as

$$W_{0,T} = \int_0^T \psi(t) d\theta(t) \quad (1)$$

however it is not certain that all of this energy is dissipated. In the case of closed loops (in the ψ - θ plane), where the system returns to its initial configuration, the identification of work done with energy dissipated can be made. For an arbitrary input variation, however, some loops will remain open, so that the dissipated energy, $D_{0,T}$ is not equal to $W_{0,T}$.

If, hypothetically, after time T an additional process returned the system to its original state, then the additional work done on the system, W_a (not all of which would be dissipated), can be used along with twice the area of all open hysteresis loops as an upper bound on $|W_{0,T} - D_{0,T}|$. Both of these quantities satisfy certain natural bounds, and will be small compared with the total work done over a time-scale on the order of one year, as in the data analysed here. The average dissipation rate, I_{av} , over the duration of the used data, will thus be estimated directly from the total work done as given by (1):

$$I_{av} \simeq \frac{1}{T} \int_0^T \psi(t) d\theta(t) \quad (2)$$

Again, errors will be introduced by supposing that variations between discrete data points take place monotonically. Variations on time-scales of less the data resolution will not be represented by the analysis here, which thus may under-estimate the total dissipation. However, the time scale of rainfall variability is usually shorter than one hour, so that higher frequencies in the natural input “signal” are aliased onto lower frequencies. The results described in *Brokate et al. (2011)* suggest that energy dissipation rates are significantly lower for high-frequency inputs than for low frequencies, so that the effect of discretisation is to over-estimate the dissipation rate. The two errors will thus offset each other to some extent, and in any event should not affect the order of magnitude of the result.

3 Results

The calculation of I_{av} from (2) was carried out by simple numerical quadrature. The resulting graphs of $W_{0,t}$ for each time series are shown in figure 9. A clear transient is seen in the results from the second, deeper, time series. This suggests that the initial memory configuration is somewhat more complicated than assumed. The transient

is quickly forgotten, however, and a similar (albeit exaggerated) profile to the first series is seen. A clear change in the behaviour can be seen in August '03, lasting for 2–3 months. This seems to be due to a sharp drying event (a dry, hot August). The effect of this drying lasts for some months — the saturation curves do not return to their previous levels until late October.

The average dissipation rate, I_{av} estimated using (2), for both series is shown in figure 10. A convergence can be seen in both data sets, at least towards the end of the data. To test this convergence, the calculation was repeated for a double-length time series formed by periodically extending the data. The change in the converged average rate was less than 10%.

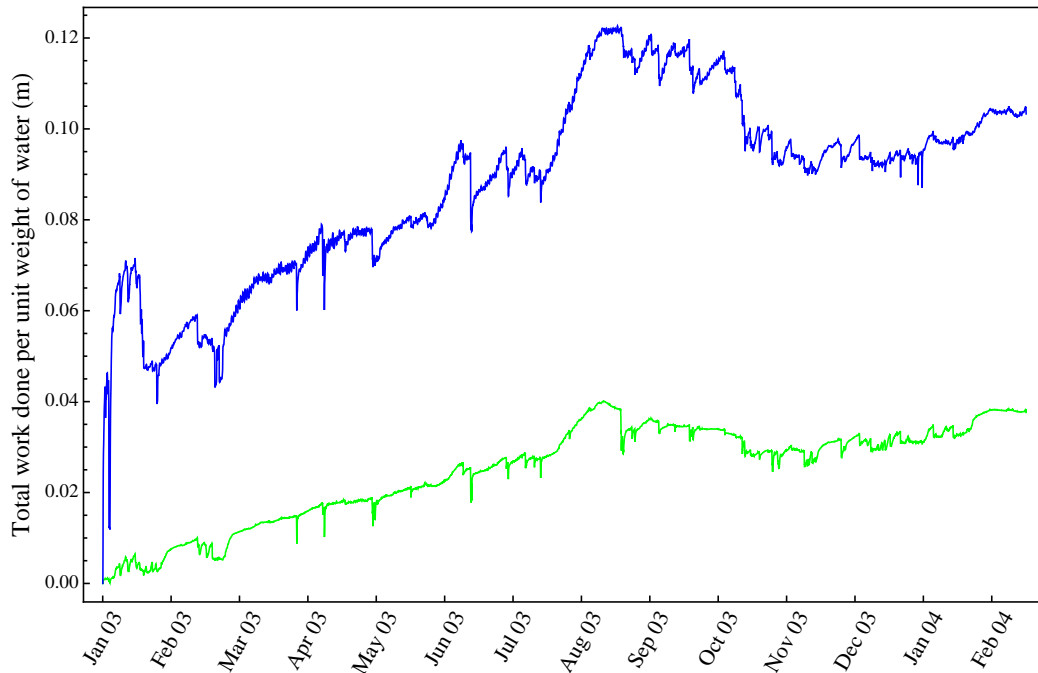


Figure 9: Total work done as a function of time, $W_{0,t}$, for the two time-series. Some transient behaviour can be seen, particularly for the deeper data (in blue). There is also a strong suggestion that a different regime takes hold from August–October. This could be explained by a period of drying, or a qualitative difference in the time-scales of wetting and drying. Since data is only available for one such season it is hard to form firm conclusions.

Some conversion is required to produce a useful figure for the average rate. The matric potential calculated in this reconstruction is measured as energy per unit weight of water, in units of m. The resulting dissipation rate is similarly given as energy per unit weight of water per hour. To convert to energy units, a conversion

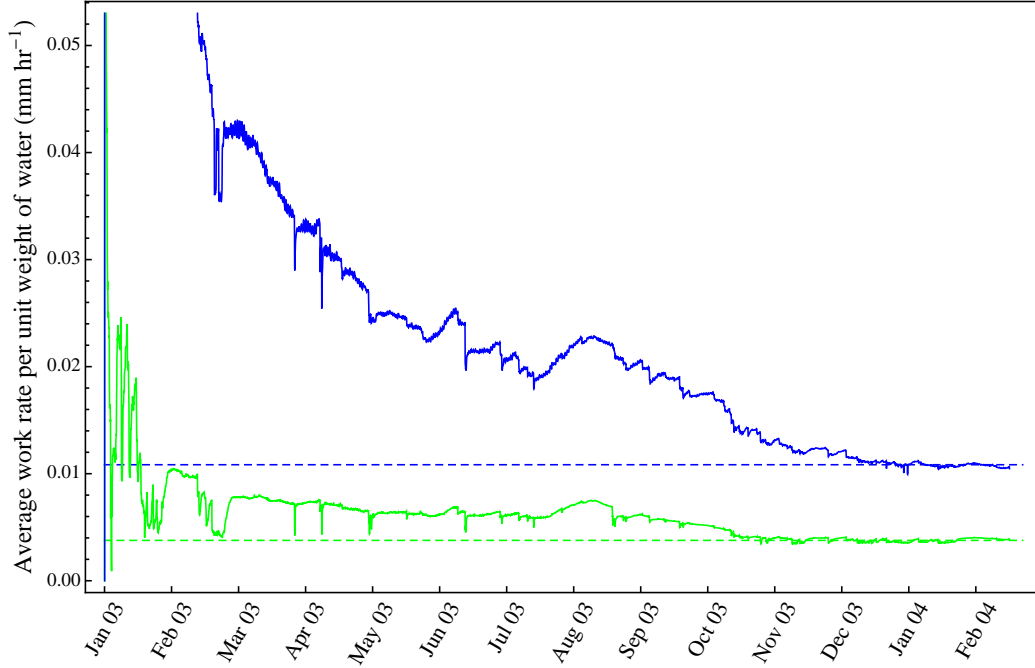


Figure 10: Average dissipation rate, I_{av} , as a function of time. Convergence to an overall average rate can be seen towards the end of the data. Dotted lines show the mean value of I_{av} over the last 2000 data points. These are the values quoted in the main text.

factor should be used. The conversion factor is given by

$$g_{conv} = \frac{\rho_w g \phi}{3600}$$

where ρ_w is the density of water, g is the acceleration due to gravity and ϕ is the porosity of the soil (fraction of the soil volume occupied by water when fully saturated). The factor of 3600 is to convert from hours to seconds. The porosity of the particular soil at the location where the data was measured is not known, and so a value must be assumed. Typical soil porosities can vary between around 0.25 and around 0.7. An intermediate value of 0.4 is used here, although it must be said that this is an entirely arbitrary choice. An order of magnitude estimate of the dissipation rate is all we expect here, so this arbitrariness can be tolerated.

The resulting dissipation rates are $3.5 \times 10^{-6} \text{ W m}^{-3}$ for the first, shallower data; and $1.1 \times 10^{-5} \text{ W m}^{-3}$ for the second data. Both of these values are consistent with the estimate of $O(10^{-5}) \text{ W m}^{-3}$ obtained in *Brokate et al. (2011)*. The deeper data set shows an increased rate of energy dissipation, which is likely due to higher variability in the saturation at this depth. Also note that the location at which this data

was obtained has a mild, wet climate characteristic of western Ireland, and the dissipation rates are likely to be quite different elsewhere. Since to the authors knowledge this is the first estimate of its kind this should not be seen as problematic, but as an incentive to perform similar analyses elsewhere.

Conclusions

To conclude, an estimate of hysteretic energy losses, made directly from soil saturation time-series, confirms the estimate from *Brokate et al.* (2011), which was made mainly on the basis of modelling. As outlined in that work, this amounts to a heating effect which is of similar magnitude to that caused at a depth of 1m by insolation. This is a significant effect, and merits both further study and consideration in the treatment of water infiltration. Of further interest would be the longer-time behaviour of this effect and its dependence on temperature and rainfall patterns. The technique used to estimate the matric potential from moisture data is also novel, although it is somewhat crude, and may find further applications.

Acknowledgements

Part of this work was carried out while the author was supported by the Oxford Martin School. The author also benefited from the hospitality of the Aspen Center for Physics, courtesy of the National Science Foundation Grant No. 1066393, and from award No KUK-C1-013-04, made by King Abdullah University of Science and Technology (KAUST). A special acknowledgement must go to the late Prof. Alexei Pokrovskii, one of the originators of the mathematical theory of hysteresis, who suggested this investigation but unfortunately did not see its completion.

References

- Appelbe, B., D. Flynn, H. McNamara, P. O’Kane, A. Pimenov, A. V. Pokrovskii, D. Rachinskii, and A. Zhezherun (2009), Rate independent hysteresis in terrestrial hydrology, *IEEE Control Systems Magazine*, 29(1), 44–69.
- Bagagiolo, F., and A. Visintin (2000), Hysteresis in filtration through porous media, *Journal for Analysis and its Applications*, 19(4), 977–997.
- Bertotti, G., and I. D. Mayergoyz (Eds.) (2006), *The Science of Hysteresis*, Elsevier Academic Press, Amsterdam.

- Brokate, M., and J. Sprekels (1996), *Hysteresis and phase transitions*, *Applied Mathematical Sciences*, vol. 121, x+357 pp., Springer-Verlag, New York.
- Brokate, M., S. MacCarthy, A. Pimenov, A. Pokrovskii, and D. Rachinskii (2011), Modelling energy dissipation due to soil-moisture hysteresis, *Environmental Modelling and Assessment*, 16(4), 313–333.
- Fisher, R. (1926), On the capillary forces in an ideal soil: correction of formulae given by w.b. haines, *Journal of Agricultural Science*, 16, 492–503.
- Flynn, D., H. McNamara, P. O’Kane, and A. V. Pokrovskii (2006), Application of the Preisach model to soil-moisture hysteresis, in *Bertotti and Mayergoyz* (2006), pp. 689–744.
- Flynn, D., O. Rasskazov, A. Zhezherun, and M. Donnegan (accessed 3 July 2012), Systems with hysteresis, <http://euclid.ucc.ie/hysteresis/>, dept. Applied Maths, University College Cork.
- Haines, W. (1927), Studies in the physical properties of soil, *Journal of Agricultural Science*, 17, 264.
- Haines, W. B. (1925), Studies in the physical properties of soils. II. A note on the cohesion developed by capillary forces in an ideal soil., *Journal of Agricultural Science*, 15, 529–535.
- Haines, W. B. (1930), Studies in the Physical Properties of Soil: V. The hysteresis effect in Capillary Properties, and the Modes of Moisture Distribution Associated Therewith., *Journal of Agricultural Science*, pp. 97–116.
- Hanyga, A., and M. Seredyńska (2005), A dynamic model of capillary hysteresis in immiscible fluid displacement, *Transport in Porous Media*, 59, 249–265.
- Haverkamp, R., P. Reggiani, P. J. Ross, and J. P. Parlange (2002), *Environmental Mechanics: Water, Mass and Energy Transfer in the Biosphere. The Philip Volume. Geophysical Monograph 129.*, chap. Soil Water Hysteresis Prediction Model Based on Theory and Geometric Scaling, pp. 213–246, The American Geophysical Union.
- Hustad, O. S. (2002), A coupled model for three-phase capillary pressure and relative permeability, *SPE Journal*, 7(1), 59–69.
- Kleppe, J., P. Delaplace, R. Lenormand, G. Hamon, and E. Chaput (1997), Representation of capillary pressure hysteresis in reservoir simulation, in *SPE Annual Technical Conference and Exhibition*, Society of Petroleum Engineers.
- Krasnosel’skii, M. A., and A. V. Pokrovskii (1989), *Systems with Hysteresis*, Springer-Verlag, Berlin.
- Krejčí, P. (1996), *Hysteresis, Convexity and Dissipation in Hyperbolic Equations*, Gakkōtoshō, Tokyo.

- Lamacz, A., A. Rätz, and B. Schweizer (2011), A well-posed hysteresis model for flows in porous media and applications to fingering effects, *Advances in Mathematical Sciences and Applications*, 21(1), 33–64.
- Mayergoyz, I. D. (1991), *Mathematical Models of Hysteresis*, Springer-Verlag, Berlin.
- Mayergoyz, I. D. (2003), *Mathematical Models of Hysteresis And Their Applications*, Elsevier, Amsterdam.
- Morrow, N. R., and C. C. Harris (1965), Capillary equilibrium in porous materials, *SPE Journal*, 5(1), 15–24.
- O’Kane, J. P., and L. Migliori (2004), The hydrology and hydraulics of a pumped polder in North Kerry: a case study in Hydroinformatics.
- Preisach, F. (1935), Über die magnetische nachwirkung, *Zeitschrift für Physik*, 94(5–6), 277–302.
- Visintin, A. (Ed.) (1993), *Models of hysteresis*, Pitman Research Notes in Mathematics, Longman Scientific & Technical.
- Visintin, A. (1994), *Differential models of hysteresis*, *Applied Mathematical Sciences*, vol. 111, Springer-Verlag, Berlin.

RECENT REPORTS

12/47	An Ensemble Bayesian Filter for State Estimation	Farmer
12/48	Simulation of cell movement through evolving environment: a fictitious domain approach	Séguis Burrage Erban Kay
12/49	The Mathematics of Liquid Crystals: Analysis, Computation and Applications	Majumdar
12/50	Fourier spectral methods for fractional-in-space reaction-diffusion equations	Bueno-Orovio Kay Burrage
12/51	Meniscal tear film fluid dynamics near Marx's line	Zubkov Breward Gaffney
12/52	Validity of the Cauchy-Born rule applied to discrete cellular-scale models of biological tissues	Davit Osborne Byrne Gavaghan Pitt-Francis
12/53	A thin rivulet or ridge subject to a uniform transverse shear stress at its free surface due to an external airflow	Sullivan Paterson Wilson Duffy
12/54	The Stokes boundary layer for a thixotropic or antithixotropic fluid	McArdle Pritchard Wilson
12/55	Thermoviscous Coating and Rimming Flow	Leslie Wilson Duffy
12/56	On the anomalous dynamics of capillary rise in porous media	Shikhmurzaev Sprittles
12/57	Compactly supported radial basis functions: how and why?	Zhu
12/58	Multiscale reaction-diffusion algorithms: pde-assisted Brownian dynamics	Franz Flegg Chapman Erban
12/59	Numerical simulation of shear and the Poynting effects by the finite element method: An application of the generalised empirical inequalities in non-linear elasticity	Mihai Goriely
12/60	From Brownian dynamics to Markov chain: an ion channel example	Chen Erban Chapman
12/61	Three-dimensional coating and rimming flow: a ring of fluid on a rotating horizontal cylinder	Leslie Wilson Duffv

12/62	A two-pressure model for slightly compressible single phase flow in bi-structured porous media	Soulaine Davit Quintard
12/63	Mathematical modelling plant signalling networks	Muraro Byrne King Bennett
12/64	A model for one-dimensional morphoelasticity and its application to fibroblast-populated collagen lattices	Menon Hall McCue McElwain
12/65	Effective order strong stability preserving RungeKutta methods	Hadjimichael Macdonald Ketcheson Verner
12/66	Morphoelastic Rods Part I: A Single Growing Elastic Rod	Moulton Lessinnes Goriely
12/67	Wrinkling in the deflation of elastic bubbles	Aumaitre Knoche Cicuta Vella
12/68	Indentation of ellipsoidal and cylindrical elastic shells	Vella Ajdari Vaziri Boudaoud
12/69	Memory of Recessions	Cross McNamara Pokrovskii

Copies of these, and any other OCCAM reports can be obtained from:

**Oxford Centre for Collaborative Applied Mathematics
Mathematical Institute
24 - 29 St Giles'
Oxford
OX1 3LB
England
www.maths.ox.ac.uk/occam**